Effects of Spatially Variable Flow on the Attenuation of Acid Mine Drainage in Groundwater

Sten Berglund[*], Maria Malmström[@], Jerker Jarsjö[#], Georgia Destouni[#]
[*]Land and Water Resources Engineering, Royal Institute of Technology (KTH),
SE-10044 Stockholm, Sweden
[@]Chemical Engineering and Technology, Royal Institute of Technology (KTH),
SE-10044 Stockholm, Sweden
[#]Natural Geography and Quaternary Geology, Stockholm University, SE-10691 Stockholm, Sweden

Abstract

Understanding and prediction of the spreading of acid mine drainage (AMD) in groundwater and the breakthrough of acidity and heavy metals downstream of waste deposits are important for risk assessments of mining sites. Quantification of both multi-component reactions and spatially variable groundwater flow is required, due to the complex geochemical characteristics of AMD and the heterogeneity of the subsurface. We use the LaSAR-PHREEQC stochastic modelling approach for reactive solute transport, and formulate and compare three alternative cases regarding groundwater flow variability and two different geochemical reaction models. We focus on the spreading of Zn^{2+}, using field data from a mill tailings impoundment in Kristineberg, northern Sweden, and include major component geochemistry. Model results indicate that Zn^{2+} could be substantially attenuated by precipitation of smithsonite, $ZnCO_3$, as one example of a heavy metal ion attenuating process. Moreover, both the groundwater flow variability and the choice of geochemical model, significantly affect the values and temporal evolution of resulting expected solute concentrations downstream of the mine waste deposit.

Introduction

The spreading of Acid Mine Drainage (AMD) in the groundwater surrounding a mine waste deposit depends on a variety of factors related to the hydrological conditions and to the (bio)geochemical processes that act to retard and transform the transported solutes. The locations of groundwater discharge areas and the associated travel times for groundwater from the deposit to the discharge area are hydrological features with possible strong implications for the effects of the reactions. Preferential flow and nonuniformity in the mean groundwater flow due to recharge may also have large effects on fieldscale contaminant spreading (cf. Simic and Destouni, 1999).

Since groundwater flow is usually highly spatially variable, different flow paths are characterised by different water residence times, even if the transport distances are similar. This implies that the times available for the reactions to affect the transported substances are different along different flow paths. Stochastic modelling provides a rational framework for handling such spatial variability and the associated prediction uncertainties in reactive subsurface solute transport. In particular, the LaSAR (Lagrangian Stochastic Advective Reactive) approach, in which transport is modelled along a set of random flow paths or streamtubes, is an efficient tool for quantifying the coupled effects of variability and reactions within a stochastic framework (Cvetkovic and Dagan, 1994).

Furthermore, a wide range of geochemical processes, e.g. pH and redox buffering, sorption, and precipitation/ dissolution processes, may affect the spreading and attenuation of AMD in groundwater. Transport models for AMD applications must therefore include a relatively comprehensive set of reactions, as compared to transport models for many other applications, and allow for testing of alternative conceptual geochemical models under realistic field conditions of spatial variability and uncertainty, with limited computational effort.

The recently developed LaSAR-PHREEQC approach (Malmström et al., 2003) provides an efficient way to model complex reaction systems in spatially variable flow fields. In this paper, we apply the LaSAR-PHREEQC approach to investigating the combined effect of geochemical processes and spatially variable flow on AMD spreading. Specifically, we focus on the transport

and attenuation of Zn^{2+}, a metal ion that commonly occurs at high concentrations in AMD, and has a relatively simple geochemistry.

Using field data from a mill tailings impoundment in Kristineberg, northern Sweden, we study Zn^{2+} attenuation under different geochemical and hydrological conditions. In particular, we investigate the effects of different degrees of spatial variability in the parameters that govern groundwater flow, including preferential flow, for two alternative geochemical models. The results are evaluated in terms of integrated solute breakthrough curves (BTCs), which illustrate the effects of spatial variability on the various "fronts" that are generated by the reaction processes.

Modelling methodology

Field-scale spreading of AMD has been investigated in a number of recent modelling studies (e.g., Bain et al., 2000; Zhu and Burden, 2001). In these studies, transport is modelled by combining a reaction model with an advective-dispersive description of mass transport in the aqueous phase. The resulting advection-dispersion-reaction equations are solved numerically in a Eulerian (x,y,z) model domain. This general and conceptually straightforward approach requires considerable computational resources when dealing with the complex reactions involved in AMD applications. The computational demand may become prohibitive in terms of including also the common spatial variability and associated model uncertainty.

The LaSAR-PHREEQC approach provides an alternative modelling framework in which complex reactions, random spatial flow variability, and uncertainty can be taken into account with limited computational effort. This approach is based on the conceptual model of a flow and transport domain resolved into a set of streamtubes. The streamtubes are characterised by individual travel or residence time for water, denoted τ, from the source (e.g., the boundary of a tailings impoundment) to the observation or control plane (CP) considered (e.g., a discharge area in the surroundings). The well-established PHREEQC code (Parkhurst and Appelo, 1999) is used to model the geochemical processes along the streamtubes; this code offers generality and flexibility to the formulation of the reaction model.

As described in more detail by Malmström et al. (2003; see also Yabusaki et al., 1998), the modelling procedure consists of two basic steps. In the first step, transport equations describing advection and reactions in a homogeneous one-dimensional domain are solved in PHREEQC to obtain concentrations along individual streamtubes, expressed as functions of time, t, and travel time, τ, where τ is given by the distance divided by the (constant) streamtube flow velocity in the PHREEQC model. Thus, the PHREEQC simulation results in a "matrix" $C_i(t,\tau)$ for each component i. In the second step, the concentration statistics that characterise solute transport in the field, consisting of a statistical ensemble of streamtubes, are evaluated by use of the probability density function (pdf) for τ. The pdf quantifies field-scale advective transport within the considered transport domain.

Depending on the transport problem at hand, the analysis can, for example, be directed towards the statistics of the local concentration values within a given control plane (Destouni and Graham, 1997), or the flux-averaged concentration in the total control plane discharge into a lake (e.g., Cvetkovic and Dagan, 1994). In the present study, we consider the field-scale, flux-averaged concentration at some arbitrary control plane within the aquifer (cf. below). This flux-averaged concentration may be quantified by statistical averaging over the relevant pdf (ergodic conditions; Dagan, 1989), as

$$\overline{C}_i(t) = \int_0^\infty C_i(t,\tau) f(\tau) d\tau \qquad (1)$$

where f is the flux-weighted pdf for advective travel time τ, and the integral is evaluated numerically.

The key to the computational efficiency of this modelling approach is the separation of reactive transport, which is modelled in a homogeneous one-dimensional model, from the spatially variable advective transport, which is expressed through the pdf. The travel time, τ, along each streamtube is then the coupling link between the two "sub models". The pdf can be quantified analytically, or

by means of numerical simulations of nonreactive transport. In some cases, the pdf can be directly evaluated from field-scale tracer data (Simic and Destouni, 1999). However, this separation of process models and the use of τ as a link between the different models also imply some limitations on the applicability of the approach. Specifically, the flow field must be steady, or uni-directional in the mean flow, and independent of the reactive processes. Furthermore, local dispersion is neglected, which implies that there is no transverse mass transport between streamtubes.

Application example

Flow and travel time variability

We formulate and compare three alternative cases regarding flow variability and corresponding variability in travel times, τ (Case 1-3, Table 1). In addition, as a reference case, we use a deterministic model of homogeneous conditions ("Case 0" in Table 1). In all three alternative cases the mean value of travel time τ, averaged over the whole CP, is the same, whereas the τ-distributions among the individual streamtubes differ. In the first two cases, we consider a relatively simple form of heterogeneity where τ follows a unimodal, log-normal pdf

$$f_{\ln}(\tau;\tau_m,\sigma)=\frac{1}{\tau\sigma\sqrt{2\pi}}e^{-\frac{1}{2\sigma^2}\left(\ln\left(\frac{\tau}{\tau_m}\right)+\frac{\sigma^2}{2}\right)^2} \quad (2)$$

where τ_m is the arithmetic mean of τ and σ is the standard deviation of $\ln\tau$. We investigate σ corresponding to modest (σ = 0.3; Case 1) and relatively high (σ = 1; Case 2) degrees of flow heterogeneity (Table 1). Although observations in many cases have supported the unimodal, log-normal formulation, it is also clear that a large fraction of the total flow and transport can take place in preferential flow paths that cannot be accounted for in a unimodal travel time pdf (e.g., Gupta et al., 1999). In order to determine the potential effect of preferential flow paths, we consider in the third case a bimodal, log-normal pdf $f_{\mathrm{bi,ln}}(\tau)$, which is a sum of two weighted unimodal pdfs, one representing the slower/normal flow paths, and the other representing the faster/preferential flow paths, according to

$$\begin{aligned} f_{bi,\ln}(\tau) &= \nu\cdot f_{\ln}(\tau;\tau_m^s,\sigma^s)+ \\ &+(1-\nu)\cdot f_{\ln}(\tau;\tau_m^f,\sigma^f) \end{aligned} \quad (3)$$

where $f_{\ln}$ is given by Equation (1), superscript s refers to the slower flow paths, superscript f refers to the preferential flow paths, and ν is the weighting factor. Note that τ_m^s of the slower/ normal flow paths and τ_m^f of the preferential flow paths in Case 3 (Table 1) were chosen such that the mean travel time of the total pdf $f_{\mathrm{bi,ln}}(\tau)$ equals 10 years as in cases 1 and 2.

Transport

We consider the reactive transport of dissolved components from a source plane at the downstream end of a tailings impoundment to a control plane (CP) at some distance L further downgradient in the mean groundwater flow direction. Specifically, we consider a distance L that is large relative to the extent of the impoundment itself, such that the heterogeneous properties of the aquifer downstream of the source will dominate system behaviour, due to its large extent relative to the source zone. Hence, we consider far-field spreading in this application example, using L = 200 m and an "effective" mean pore water velocity of 20 m/year, such that the mean advective travel time corresponding to this mean velocity is 10 years.

For instance, in a homogeneous system, a pore water velocity of 20 m/year can be the result of a hydraulic gradient J of 1%, a hydraulic conductivity K of 6×10^{-6} m/s and a flow porosity n_e of 0.1. However, it should be noted that it is the travel time statistics that constitute the hydrological input to the model. Consequently, the results presented in the following are valid for any combinations of L and flow velocity fields that yield the same travel time statistics as in Table 1.

Geochemistry

We consider the spreading of an AMD plume in anoxic, but non-reducing, generic groundwater. For illustrative purposes, we use an AMD composition that corresponds to the groundwater in one of the mill tailings impoundments at the Kristineberg sulphide ore mine in northern Sweden

prior to remediation (Table 2). We assume that the groundwater in the domain prior to contamination is, for simplicity, pure water with 2×10^{-5} M sulphuric acid acidity in equilibrium with calcite (pH 8.3) and maintain the partial pressure of carbon dioxide at the atmospheric level, $P_{CO_2} = 3\times10^{-4}$ atm.

We focus on the transport and attenuation of Zn^{2+}, a metal ion that commonly occurs at high concentrations in AMD. We also include relevant major-component geochemistry and assume that all reactions are maintained at geochemical equilibrium. We assume, for simplicity, that calcite is the only primary mineral that provides buffering capacity to the groundwater, and use an arbitrarily set calcite content of 0.3 moles per litre of soil solution.

We consider dissolution of calcite and secondary minerals to neutralise the acidity in the AMD plume. In the model, the dissolution and depletion of calcite (pH 7.9), smithsonite (pH 7.0), and siderite (pH 6.4), hence, buffer pH at successively lower levels with time. The geochemical model and its implementation in the PHREEQC code (Parkhurst and Appelo, 1999) are described in detail by Malmström et al. (2003).

Speciation calculations show that, of the Zn^{2+}-containing minerals rated by Nordstrom and Alpers (1999) as "likely to control metal concentrations" in AMD-environments, smithsonite, $ZnCO_3$, may become oversaturated in the AMD-plume. Therefore, we investigate the potential effect of precipitation of this secondary phase on the expected BTC for Zn^{2+} at the CP. The formation of siderite, through reaction between dissolved ferrous iron in the AMD plume and calcite in the groundwater,

$$\mathrm{CaCO_{3(s)} + Fe^{2+} + SO_4^{2-} + 2H_2O \Leftrightarrow FeCO_{3(s)} + CaSO_4 \times 2H_2O_{(s)}} \qquad (4)$$

may decrease the attenuation of Zn^{2+} through, e.g., the lower pH at which siderite buffers pH, compared to calcite. However, although thermodynamically favoured, the formation of siderite from calcite and dissolved ferrous iron may be slow, or may not even occur at all in the groundwater system. Thus, we consider two limiting cases where reaction 4 is either kept at geochemical equilibrium (Case A) or considered not to occur (Case B).

Results

Figure 1 shows the BTC for the limiting case where reaction 4 is allowed to reach geochemical equilibrium (Case A) and where a unimodal pdf for travel time τ is considered. The step-like appearance of the sulphate concentration in the deterministic model (blue curve in Figure 1a) is due to retardation of sulphate through reaction 4. In the presence of calcite, this reaction is limited by the availability of dissolved ferrous iron in the plume; thus, excess sulphate (0.02 M) is mobile and breaks through at $t = \tau_m$. Due to depletion of calcite up to our CP, the sulphate concentration increases considerably at $t \approx 44$ years. Subsequent redissolution of gypsum causes the concentration of sulphate to exceed that of the source AMD somewhat throughout the simulation. The small peak in the sulphate concentration around 44 years is due to the breakthrough of Zn^{2+} at this point (compare Figure 1b), and the higher solubility of sulphate in the presence of Zn^{2+}.

Figure 1a furthermore illustrates that the step in sulphate concentration due to reaction 4 in the deterministic case (blue line) will be almost completely masked in heterogeneous flow fields (green and purple lines), already for low travel time variability ($\sigma = 0.3$; green line). This retardation may therefore be hard to distinguish from, e.g., retardation due to pure sorption, on the basis of measured concentrations at the CP alone. It also seen in Figure 1 that this "smoothing" of the BTC increases with increasing flow heterogeneity.

For the deterministic model, only a small fraction (~1/10) of the Zn^{2+} in the source AMD breaks through at $t = \tau_m$. This is due to precipitation of smithsonite in the groundwater and the associated retardation of Zn^{2+}. However, smithsonite is only stable in the presence of calcite, and redissolves at the calcite depletion front, causing a peak in the Zn^{2+} concentration at the CP after ~44 years. For the deterministic model, the peak concentration of Zn^{2+} exceeds that of the source AMD with a factor of as much as ~15. After depletion of all smithsonite, caused by redissolution during ~2 years, the Zn^{2+} concentration equals that in the source AMD.

However, Figure 1b also shows that the peak concentration of Zn^{2+} is a factor 9 lower in the mildly heterogeneous case (green line) than in the deterministic case (blue line), and the difference increases with increased heterogeneity (purple line). This implies that the peak concentration predicted by the homogenous model is irrelevant already in flow fields with a relatively low degree of heterogeneity. Moreover, larger travel time variability implies much higher concentrations of Zn^{2+} prior to the breakthrough predicted by the deterministic model (t < 44 years in Figure 1).

Figure 2 shows a comparison of the BTCs with and without presence of preferential flow paths (red and green curve, respectively), considering the model where siderite is forming and dissolving. Note that the unimodal curve in Figure 2b (σ=0.3; Case 1) is the same as in Figure 1b, although the scale is magnified. As expected, the first arrival of both sulphate and Zn^{2+} is faster with preferential flow. However, a less obvious effect of preferential flow is that the local minimum in the Zn^{2+}-curve in the presence of preferential flow paths approximately coincides in time ($t \approx 50$ years in Figure 2b) with the maximum Zn^{2+} concentration that occurs without preferential flow (Case 3).

Figure 3 compares the results for our two different geochemical cases, i.e., calcite to siderite transformation is maintained at equilibrium (Case A; green line) or assumed not to occur (Case B; pink line) for a unimodal pdf with modest travel time variability (σ = 0.3; Case 1). For Case B, sulphate is attenuated through precipitation of gypsum. This reaction is, for our conditions, limited by the rate of calcite dissolution, which, in turn is dominated by the rate of acidity supply, where aluminium acidity is dominating in the source AMD,

$$3\mathrm{CaCO}_{3(s)} + \mathrm{A}lSO_4^+ + 2SO_4^{2-} + 9H_2O \quad \Leftrightarrow$$
$$3\,\mathrm{CaSO}_4 \times 2\mathrm{H}_2\mathrm{O}_{(s)} + Al(OH)_{3(am)} + 3HCO_3^- \quad (5)$$

Sulphate, hence, breaks through at a concentration somewhat lower than in the source AMD and remains at this level throughout the simulation.

For both cases, Zn^{2+} breaks through at similar, low concentration. In Case B, as opposed to Case A, a low concentration is maintained throughout the simulation. The small increase in Zn^{2+} concentration that starts to occur after 100 years signifies depletion of calcite and remobilisation of Zn^{2+} in some of the streamtubes.

Discussion and conclusions

The presented results have several implications for risk assessments associated with mine waste sites. Firstly, model results indicate that, under the considered geochemical conditions, Zn^{2+} may be substantially attenuated on its path from the mine waste deposit towards a downstream compliance boundary or some sensitive water recipient through precipitation of smithsonite, as one example of a heavy metal ion attenuating process, reducing the Zn^{2+} concentration by up to about one order of magnitude over decades. However, if the contamination continues over longer time, thereby causing depletion of calcite in the groundwater system and associated transition to lower pH, attenuated Zn^{2+} may be remobilised and cause a peak load of this heavy metal.

Secondly, increased travel time variability implies, irrespectively of the type of pdf considered, a longer duration but a lower maximum concentration of Zn^{2+} in the peak associated with redissolution of smithsonite. In fact, the homogeneous (deterministic) model predicts peak concentrations of Zn^{2+} that are not within the right order of magnitude, even if field conditions are characterised by only a low degree of flow heterogeneity. Moreover, travel time variability also implies that a considerable concentration of Zn^{2+} may reach the CP relatively early (at $t < \tau_m$). This means that smithsonite may not be as efficient in attenuating Zn^{2+} as standard, deterministic reactive transport modelling would indicate. Interestingly, these peak concentrations of Zn^{2+} occur long before a drop in pH from near-neutral values is expected (not shown). This indicates that expected or measured pH may be a poor indicator for metal mobility in the groundwater system, and the risk of heavy metal breakthrough.

We also show that even a low degree of flow heterogeneity can effectively smooth otherwise distinctive temporal concentration changes attributed to the onset of a chemical reaction, resulting in breakthrough curves that are similar to, e.g., sorbing solutes in homogeneous media. As expected, the presence of preferential flow paths implied

earlier solute breakthrough. Interestingly, in our case of preferential flow, concentrations actually reached a temporal minimum subsequent to peaking. This illustrates that spatial variability in flow may have effects that easily could be attributed to the geochemical processes, making the interpretation of the BTC non-trivial.

Furthermore, we compared two cases where calcite to siderite formation and redissolution of siderite was considered either not to occur or to be maintained at geochemical equilibrium, with these cases representing uncertainty in the dominant geochemical processes that need to be considered in models. The observed large difference in Zn^{2+} BTC between these two cases highlights the necessity of accurate selection and quantification of processes required in transport modelling, based on detailed site characterisation, including travel time distribution and mineralogical determinations (cf. Zhu and Burden, 2001).

The results presented in this communication emphasise the importance of the interactions between hydrology and geochemistry for field-scale AMD spreading. We believe that the LaSAR-PHREEQC approach provides an efficient means for further investigations of these coupled processes and their effects.

Acknowledgement

This research was partly funded by the Swedish Foundation of Strategic Research (MISTRA) through the research programme "Mitigation of the environmental impact from mining waste" (MiMi).

References

Bain, J.G., Blowes, D.W., Robertson, W.D., Frind, E.O. 2000. Modelling of sulfide oxidation with reactive transport at a mine drainage site. J. Contam. Hydrol., 41, 23-47.

Cvetkovic, V., Dagan, G. 1994. Transport of kinetically sorbing solute by steady random velocity in heterogeneous porous formations. J. Fluid Mech., 265, 189-215.

Dagan, G. 1989. Flow and transport in heterogeneous formations. Springer-Verlag, New York.

Destouni, G., Graham, W. 1997. The influence of observation method on local concentration statistics in the subsurface, Water Resour. Res., 33, 663-676.

Gupta, A., Destouni, G. and Jensen, M.B. 1999. Modelling tritium and phosphorous transport by preferential flow in structured soil. J. Contam. Hydrol., 35, 389-407.

Malmström, M.E., Werner, K., Salmon, U., Berglund, S. 2001. Hydrogeology and geochemistry of mill tailings impoundment 1, Kristineberg, Sweden: Compilation and interpretation of pre-remediation data. MiMi Report 2001:4, MiMi programme, Stockholm, Sweden.

Malmström, M.E., Destouni, G., Martinet, P. 2003. The LaSAR-PHREEQC approach to modelling solute concentrations in heterogeneous flow systems with multi-component reactions. (Manuscript in preparation.)

Nordstrom, D.K., Alpers, C.N. 1999. Geochemistry of acid mine waters. P133-160. *In* Plumlee, G.S., Logsdon, M.J. (Eds), Environmental geochemistry of mineral deposits, Reviews in Economic Geology 6A, Soc. Ec. Geologists, Chelsea, USA.

Parkhurst, D.L., Appelo, C.A.J. 1999. User's guide to PHREEQC (version 2) USGS Water-Resources Investigations Report 99-4259, USGS, Denver, Colorado, USA.

Simic, E., Destouni, G. 1999. Water and solute residence times in a catchment: Stochastic-mechanistic model interpretation of ^{18}O transport. Wat. Resour. Res., 35, 2109-2119.

Yabusaki, S.B., Steefel, C.I., Wood, B.D. 1998. Multidimensional, multicomponent, subsurface reactive transport in nonuniform velocity fields: code verification using an advective reactive streamtube approach. J. Contam. Hydrol., 30, 299-331.

Zhu, C., Burden, D.S. 2001. Mineralogical composition of aquifer matrix as necessary initial conditions in reactive contaminant transport models. J. Contam. Hydrol., 51, 145-161.

Table 1. Considered hydrological conditions.

Case	pdf for τ	Parameter values
0	*	$\tau = 10$ years
1	Eqn (2)	$\sigma = 0.3$, $\tau_m = 10$ years
2	Eqn (2)	$\sigma = 1$, $\tau_m = 10$ years
3	Eqn (3)	$\sigma^s = \sigma^f = 0.3$; $\tau_m^s = 22.7$ yrs, $\tau_m^f = 4.54$ years, $\nu = 0.3$

*Homogeneous conditions (a single value of τ)

Table 2. Groundwater composition in Impoundment 1, Kristineberg, Sweden, prior to remediation, as compiled by Malmström et al. (2001).

Component	Concentration [M]
SO_4^{2-}	0.10
Fe(II)*	0.080
Zn^{2+}	0.0060
Ca^{2+}	0.0050
Mg^{2+}	0.011
Al	0.0020
pH	4.9

*For this modelling purpose, we only consider ferrous iron.

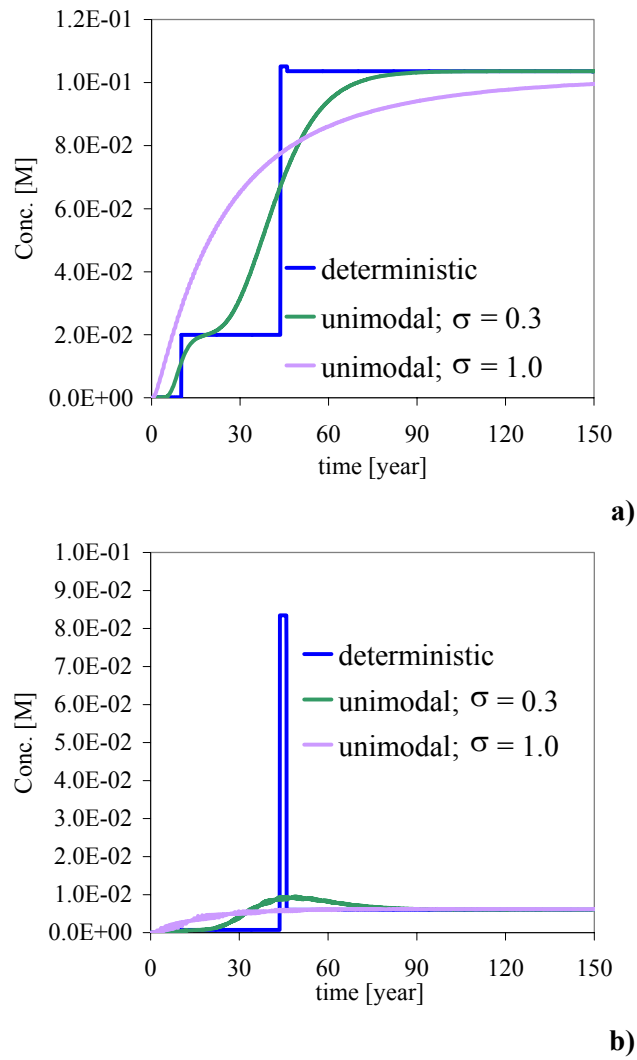

Figure 1. Modelled BTCs assuming formation and redissolution of siderite (Case A) and a unimodal pdf with τ_m =10 years. **a)** SO_4^{2-}; **b)** Zn^{2+}. Blue line - deterministic model. Green line - medium travel time variability (σ = 0.3; Case 1). Purple line – relatively high travel time variability (σ = 1.0; Case 2).

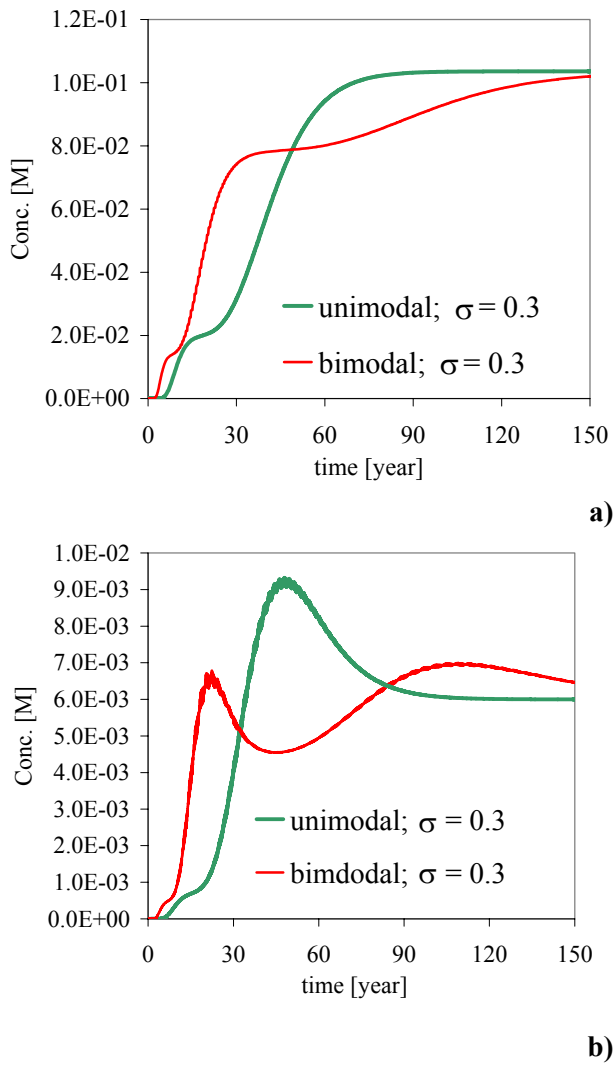

Figure 2. Modelled BTCs assuming formation and redissolution of siderite (Case A) for different travel time distributions with τ_m =10 years and σ = 0.3. **a)** SO_4^{2-}; **b)** Zn^{2+}. Green line – unimodal pdf (Case 1). Red line – bimodal pdf (Case 3).

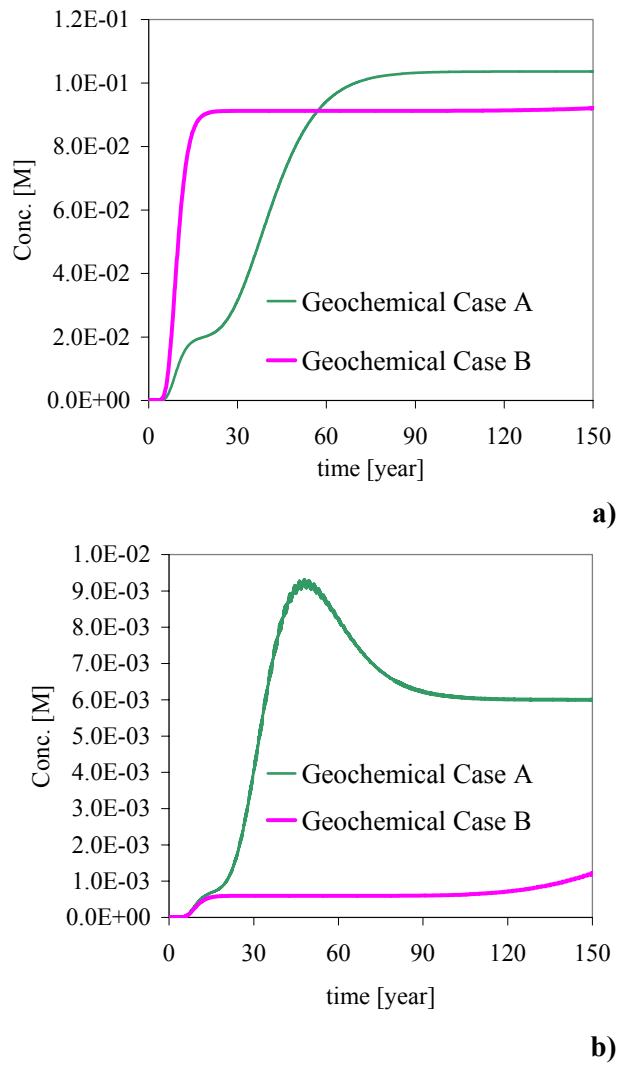

Figure 3. Modelled BTCs for the two geochemical models and a unimodal pdf with τ_m =10 years and σ= 0.3 (Case 1). **A)** SO_4^{2-}; **b)** Zn^{2+}. Green line – siderite at equilibrium (Case A). Pink line – siderite formation and redissolution not considered (Case B).